frontiers | Frontiers in Materials

ORIGINAL RESEARCH
published: 05 May 2022
doi: 10.3389/fmats.2022.892765

Grain Size and Macrosegregation Control of Large-Sized AA2219 Billets by Internal Electromagnetic Stirring in DC Casting

Haodong Zhao[1,2,3], *Zhifeng Zhang*[1,2,3]*, *Bao Li*[1,2,3]*, *Yuelong Bai*[1,2,3] and *Mingwei Gao*[1,2,3]

[1]National Engineering & Technology Research Center for Non-ferrous Metal Composites, GRINM Group Co., Ltd., Beijing, China, [2]GRINM Metal Composites Technology Co., Ltd., Beijing, China, [3]General Research Institute for Nonferrous Metals, Beijing, China

This work focuses on the effect of internal electromagnetic stirring (IEMS) on grain size and macrosegregation in direct-chill (DC) casting of an AA2219 billet with a diameter of 880 mm. The IEMS process has been applied to provide forced convection within the solidifying melt to achieve an efficient reduction of mean grain size and alleviate the formation of macrosegregation. Two casting electromagnetic parameters (the stirring electric current and frequency) of the IEMS process were applied to assess the uniformity of the microstructure and macrosegregation of the billet. The experimental results show that finer and more uniform grains in the billet prepared by the IEMS process than those of traditional DC casting have been observed. The IEMS process has a great influence on the improvement of the macrosegregation, but the greater electromagnetic field would result in worse macrosegregation in the center of the billet.

Keywords: grain size, macrosegregation, 2219 aluminum alloy, large-sized billets, internal electromagnetic stirring, DC casting

OPEN ACCESS

Edited by:
Zhilin Liu,
Central South University, China

Reviewed by:
Lei Li,
Northeastern University, China
Xiangjie Wang,
Northeastern University, China

***Correspondence:**
Zhifeng Zhang
zhangzf@grinm.com
Bao Li
libao@grinm.com

Specialty section:
This article was submitted to Structural Materials, a section of the journal Frontiers in Materials

Received: *09 March 2022*
Accepted: *06 April 2022*
Published: *05 May 2022*

Citation:
Zhao H, Zhang Z, Li B, Bai Y and Gao M (2022) Grain Size and Macrosegregation Control of Large-Sized AA2219 Billets by Internal Electromagnetic Stirring in DC Casting. Front. Mater. 9:892765. doi: 10.3389/fmats.2022.892765

INTRODUCTION

2219 Al alloy has the advantages of low density, high strength, excellent weldability, and high- and low-temperature mechanical properties and has been widely applied in the aerospace, aviation, and military fields (Jha et al., 2009; An et al., 2012). The large-scale AA2219 billets are usually used to manufacture vital components such as the launch vehicle storage tank transition ring. However, there are many inherent defects, such as Al_2Cu coarse second phase particles and poor uniformity of grains in the manufacturing process, which affect the mechanical properties and its uniformity (Mao et al., 2020). Therefore, a fine and uniform microstructure across the large-scale billets is much desired because it can reduce the porosity, subsequent processing difficulty, and improve the mechanical properties of the large forged ring. In the DC casting, the solidification starts from the periphery to the center of the billet due to the cooling system, resulting in a deep and sharp sump in the billet. As the size of the billet increases, the sump becomes deeper and the temperature gradient within the billet becomes larger, resulting in a coarser as-cast structure and more serious macrosegregation. To refine the structure and alleviate macrosegregation, the addition of grain refiners is used in DC casting. However, adding the grain refiners, typically TiB_2 or TiC additions, cannot eliminate the structural nonuniformity in the cross-section of the billet caused by the wide variety of cooling rates in DC casting, and it is limited to solve the macrosegregation. The application of external fields has attracted more attention, such as intensive melt shearing (Liu et al., 2019; Liu

et al., 2021), ultrasonic field (Subroto et al., 2020; Tonry et al., 2020; Zhang et al., 2021), electromagnetic field (Vives and Ricou, 1985; Mapelli et al., 2010), and the combined magnetic fields (Zhao et al., 2014; Zuo et al., 2015). For a melt shearing method or an ultrasonic field, the grain refinement is good but limited by the small action zone during the large-size billet casting. Electromagnetic stirring provides an attractive and contactless method to control the melt flow inside the liquid sump, which means the grain size and macrosegregation control can come true, although the exact mechanism is not well understood.

A great number of studies have already been reported concerning the impact of electromagnetic fields on grain size and macrosegregation in DC casting. As the earliest industrial application of the field, the electromagnetic casting (EMC) process has achieved the grain refinement of AA2024 alloys (Cao et al., 2002). And Vives (1989) proposed the CREM (casting, refining, electromagnetic) process in which the melt is stirred in a mold surrounded by a coil with a 50-Hz alternating current. A low-frequency electromagnetic casting (LFEC) process (Zhang et al., 2003; Wang et al., 2011; Zuo et al., 2014) has been developed, and the frequency was further decreased to improve the penetration ability. However, it was too difficult to cast the large-scale billets due to their proximity effect and skin effect. As the diameter increased to over 500 mm, electromagnetic stirring is only the workpiece near the outer skin, and the stirring intensity at the billet center is small, which makes the grain refinement limited. Recently, the uniform direct chill (UDC) process coupled with electromagnetic stirring and an in-mold cooler together has been proposed and achieved a good grain refining effect while producing Φ508 mm 7005 and 2219 alloy billets (Luo et al., 2017; Luo et al., 2018; Qiu et al., 2018; Luo and Zhang, 2019). And it is found that a combination of electromagnetic stirring and intercooling reduces the grain size significantly. Based on the UDC casting, the internal electromagnetic stirring (IEMS) method has been proposed by Qiu et al. (2019). In this method, the coils are placed in the in-mold cooler, and Lorentz force arises from the in-mold cooler and forces the melt to stir. The experimental results demonstrate that the periphery and center microstructures of the 2219 aluminum alloy billet with a diameter of 630 mm prepared by the IEMS process are both fine and uniform, and the macrosegregation is also significantly improved, compared with the traditional DC billet. However, there are some defects in the system of the IEMS process for casting larger billets in industrial manufacturing, and the process still needs to be perfected.

Therefore, an improved IEMS process to produce a larger aluminum alloy billet with a diameter of 880 mm is proposed in the present work. Two casting electromagnetic parameters (the stirring electric current and frequency) of IEMS were applied to assess the uniformity of microstructure and macrosegregation of the billet. The effect of IEMS on grain size and macrosegregation in DC casting of an AA2219 billet with a diameter of 880 mm was systematically analyzed, and the mechanism for improving macrosegregation was discussed to provide a basis and reference in developing the IEMS process of large-sized aluminum alloy billet.

MATERIALS AND METHODS

Figure 1A shows a schematic diagram of a DC casting process performed in the presence of the IEMS process which comprises a mold of an internal diameter of 880 mm and a 340 mm diameter in-mold electromagnetic cooler, as shown in **Figures 1A, B**, a hot top of internal diameter and height of 860 and 250 mm, respectively. An electromagnetic stirrer is embedded in the experimental in-mold electromagnetic cooler and is composed of one round yoke and nine copper induction coils. Each induction coil consists of 100-turn copper wires, and the phase shift between adjacent coils is 120° to provide the alternating magnetic field. The experimental in-mold electromagnetic cooler is filled with a circulation cooling medium to chill the coils, and the tube structures of the cooler are multiple-layer structures: the inner steel barrel, the steel outer barrel, and the thermal insulation layer. The thermal insulation materials are filled in the two separate decks of steel plate barrels to reduce heat transfer between the melt and the cooler. The 2219 aluminum alloy was employed as the experimental material in the present work, whose solidification thermal range is 543–643°C. AA2219 was prepared by melting 99.7% commercially pure aluminum, commercially pure Cu, Al-10Mn, Al-10Ti, Al-10V, and Al-4Zr master alloys in a medium-frequency induction furnace at 755 ± 5°C. The chemical composition of the AA2219 melt in the present work is given in **Table 1** and all the chemical compositions described are in weight percent (wt.%). The melt was degassed twice for 15 min each, and then was poured into a DC casting machine through a filter tank and a long launder. And a grain refiner was added online to the melted aluminum at a speed of 950 mm/min in the form of two Al-5Ti-B rods.

A round AA2219 billet up to 2800 mm in length was cast in a DC casting facility at Xinjiang Joinworld Company Limited. To obtain the observed billet, the billet was produced at a casting speed of 26 mm/min, second cooling water flow rate of 26 m^3/h, and a temperature of 710 ± 5°C. To study the revolution in the microstructure and the macrosegregation of the billet prepared in the presence of the IEMS process, the billet was sequentially produced under different conditions. After the steady-state was reached, a sufficient length of the billet (over 500 mm) was cast as a traditional billet. And then the preheat in-mold electromagnetic cooler was arranged gently inside the melt at the designated height and started to work with the intercooling medium flow rate of 20 L/min. During the IEMS process, the current intensity was imposed at 22 A and the current frequency was kept at 20 Hz under the conditions of other casting parameters remaining unchanged. When 500 mm in the length of the billet was cast, the current intensity was increased to 42 A and then another 500 mm of the billet was cast. To illustrate the effect of the current frequency, the rest of the billet was cast under the following conditions: the current intensity, 42 A; the current frequency, 30 Hz. The electromagnetic casting parameters of the processes are given in **Table 2**. At the end of the cast, the in-mold electromagnetic cooler was taken off and the cast entered its final stage. The temperature curves were measured at the positions as shown in **Figure 1** by using thermocouples during the casting process. The sump depths were measured at the end of the four processes by using a drill rod. A steel rod was probed into the melt to touch the solidification zone at different positions along the radius of

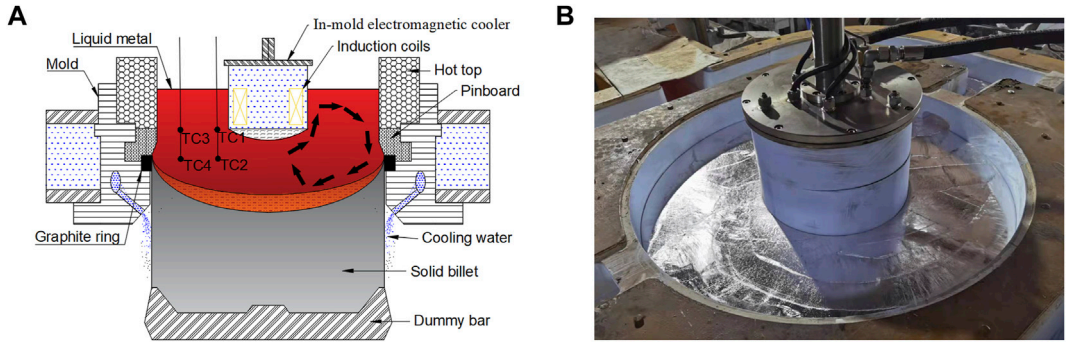

FIGURE 1 | (A) Schematic diagram of the DC casting process performed in the presence of IEMS process and temperature measurements; **(B)** the experimental in-mold electromagnetic cooler in the DC casting.

TABLE 1 | Chemical composition of the experimental 2219 aluminum alloy (wt.%).

Cu	Mn	Ti	Zr	V	Zn	Si	Fe	Al
6.20	0.32	0.07	0.20	0.10	0.02	0.03	0.06	Bal.

TABLE 2 | The electromagnetic casting parameters of the four cases.

Case	Current/A	Frequency/Hz	Casting length/mm
Traditional DC casting	0	0	600
The IEMS case 1	22	20	500
The IEMS case 2	42	20	500
The IEMS case 3	42	30	500

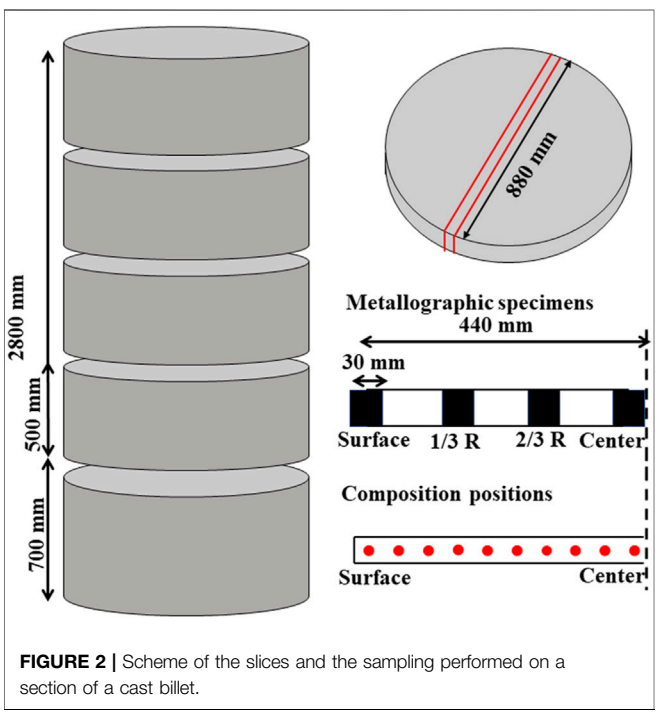

FIGURE 2 | Scheme of the slices and the sampling performed on a section of a cast billet.

the billet, and the sump depth at this location was obtained by measuring the length of the immersion. The sump depth at the center of the billet was simply calculated by measuring the length of the immersion and the immersion location in a right triangle. The billet was homogenized at 515°C for 12 h and 525°C for 26 h.

To compare and analyze the solidification characteristics of the four processes and reveal the microstructure evolution, the billet was sawed into slices at different lengths, corresponding to the steady-state stage of the aforementioned four processes, which takes about 120 mm in length to reach a steady state. The metallographic specimens prepared under different processes were cut-off along a diameter of the cross-sections. Speciments under the different process conditions were featured by square shape (30 mm × 30 mm) at four radial positions: billet surface, 1/3 radius, 2/3 radius, and center as shown in **Figure 2**. After being mechanically ground and polished, the specimens were treated with anodic coatings at 30 V direct current for 1 min in 2.5 vol.% HBF_4 in water solution. And the color metallography was observed using an Axiovert 200 MAT polarized light microscope (Zeiss). The grain size was analyzed using the linear intercept method with over 350 intercepts to obtain the soundness of this data. Meanwhile, to understand the effect produced by the electromagnetic stirrer on the macrosegregation, the chemical compositions at different positions along the radius of cross-section slices were determined by a Foundry-Master Pro direct reading spectrometer (Oxford Instruments, Oxford, United Kingdom). The specimens of chemical compositions were taken every 25 mm, starting from the surface of the billet. The three points of measurement were performed in the same position, and the results were averaged. The absolute error for copper concentration was ±0.1 wt.%

RESULTS

Microstructure of AA2219 Billet in Different Internal Electromagnetic Stirring Conditions

Figure 3 illustrates the microstructural evolution regarding variant casting electromagnetic parameters of the IEMS

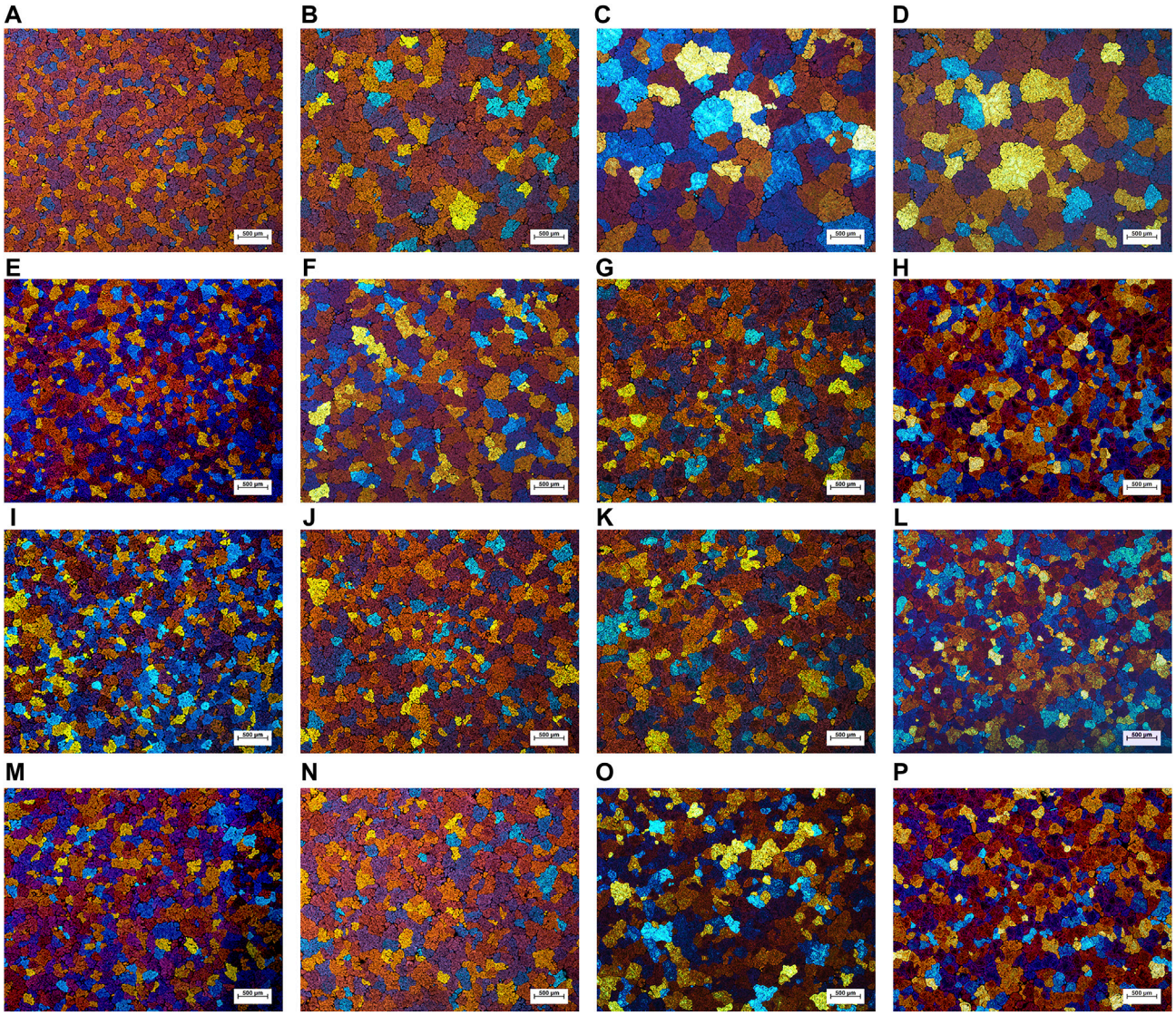

FIGURE 3 | Microstructure of an AA2219 billet with a diameter of 880 mm produced under different casting conditions: **(A**,**B**,**C**,**D)** traditional DC casting, **(E**,**F**,**G**,**H)** IEMS case 1, **(I**,**J**,**K**,**L)** IEMS case 2, **(M**,**N**,**O**,**P)** IEMS case 3; **(A**,**E**,**I**,**M)** surface, **(B**,**F**,**J**,**N)** 1/3 radius, **(C**,**G**,**K**,**O)** 2/3 radius, and **(D**,**H**,**L**,**P)** center.

process. In the traditional DC casting, the grains are rather coarse than nonuniformly distributed at the surface and the central portion of the billet. The grains at the edge have developed a dendritic morphology. And some of the grains in the center of the billet are larger with large dendritic arm spacing and thick dendritic arm, while some are much smaller. The average grain size of different casting conditions was quantified in **Figure 4** to reveal the uniformity of the grain structure on the cross-section of the billet. In general, the average grain size increases from the surface to the central portion of the billet. As can be noted, the grain size is around 282 μm at the edge and about 794 μm at the center of the traditional billet. The application of the IEMS process shows much finer and more uniform grains in the polarized light optical micrographs compared to that of the traditional DC casting. The results show that the microstructure is transformed from dendritic grains to a fine equiaxed structure in the center of the billet under the IEMS case 1. The structure comprises fine equiaxed grains and is generally uniform across the cross-section of the billet. The grain size in the central portion of the billet decreased from 794 μm in the traditional billet to around 225 μm in the billet of the IEMS case 2.

All three process parameters resulted in a significant decrease in the grain size. For the applied current intensity of 22 A, the grain structure in the central portion of the billet is quite fine with an average grain size of 293 μm. With the increase of the applied current intensity in the DC casting, the morphology of the grains appears to transition to the finer equiaxed grain region. By increasing the applied current intensity to 42 A, the grain size at the same position has no

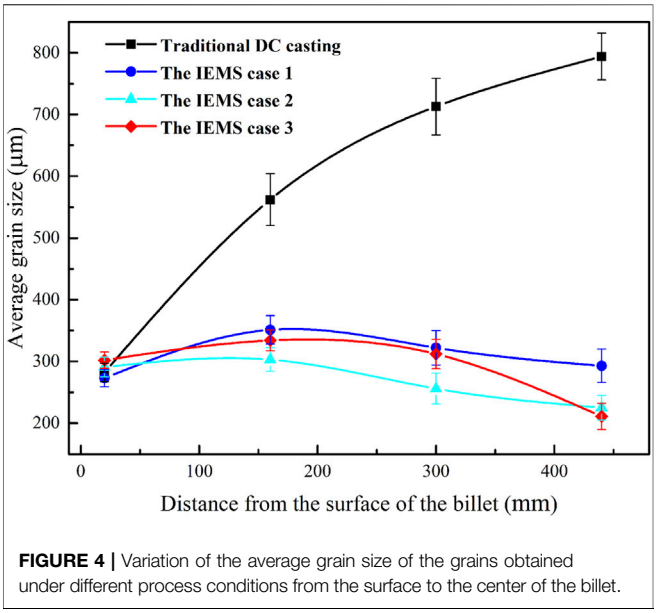

FIGURE 4 | Variation of the average grain size of the grains obtained under different process conditions from the surface to the center of the billet.

significant differences detected in the structure, but it encourages the formation of a more equiaxed structure and is drastically finer with an average grain size of 225 μm. The reduction of grain size at the edge due to the current intensity in the IEMS process is not as significant as its reduction in the center. By increasing the current frequency to 30 Hz, the structure in the central portion of the billet remains equiaxed morphology, and the grain size has decreased by almost 6%. Among the three different IEMS processes, the finest and most uniform grain structure was observed in the billet obtained with a current intensity of 42 A and a frequency of 20 Hz.

Macrosegregation Profiles of AA2219 Billet in Different Internal Electromagnetic Stirring Conditions

Experimentally measured concentrations of Cu alloy under all conditions along the billet diameter are illustrated in **Figure 5**. The relative deviation of Cu concentration from the average, ΔC, is represented in the following equation (Eskin, 2008):

$$\Delta C = \frac{C_i - C_0}{C_0} \times 100\%,$$

where C_i is the mean composition of the Cu alloy element at a specific position, and C_0 is the average alloy composition. There is obvious inverse segregation near the billet surface for all four processes and different distributions of Cu alloy elements in the central portion of the billet. It is difficult for the IEMS process to dramatically change the surface inverse segregation because the application of an internal electromagnetic field has few significant contributions to the formation of the shrinkage-induced flow. But the thin layer of surface segregation is easier and necessary to be scalped before the follow-up process, so it is not crucial in DC casting.

The macrosegregation is a key factor in determining the metallurgical qualities of the billet. It determines not only the homogeneity of the composition but also the mechanical properties of the wrought products. Among the four processes, the traditional DC casting leads to the most serious positive segregation in the central portion of the billet. In the center of the three billets prepared by the IEMS process, positive segregation does not exist, and various degrees of negative segregation take place. Therefore, the variation of center segregation by the IEMS process is very significant for large-size billet, and it perhaps provides an effective way where we can put the segregation under control by adjusting the parameters of the IEMS. As shown in **Figure 5**, due to the weaker forced convection in the sump, the billet cast by applying the current intensity of 22 A has a decrease in the negative segregation compared to the billet prepared by applying the current intensity of 42 A. The change in current frequency from 20 to 30 Hz does not affect the general distribution of the Cu alloy element in the center of the billet. The increasing current frequency of the IEMS at the same casting condition tends to produce a slight segregation in the central portion of the billet.

DISCUSSION

Coarse and nonuniform grains observed in the large-sized 2219 aluminum alloy billet are, in general, a common defect that significantly affects the quality of the final product. The microstructure shows that the grain size tends to coarsen from the periphery to the center of the billet without the IEMS process. The application of the IEMS resulted in significant grain refinement of the large-sized AA2219 billet. The alternative current in the in-mold cooler generates a time-varying magnetic field in the melt, and an induced current emerges in

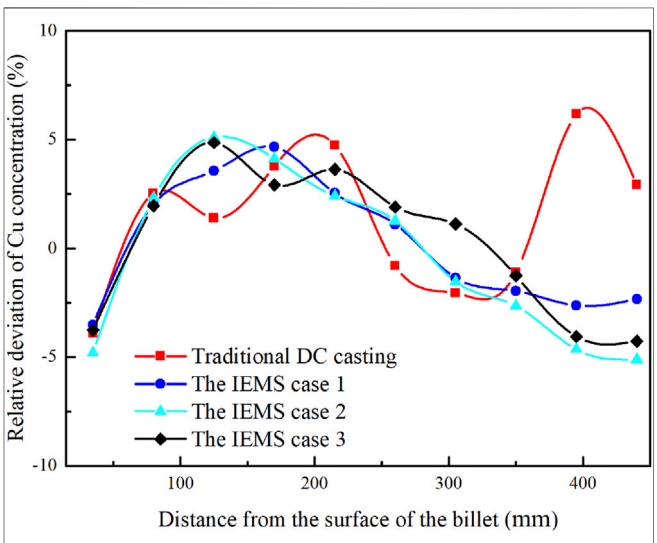

FIGURE 5 | Relative deviation of Cu concentration from the average in the radial direction of billet obtained under different process parameters.

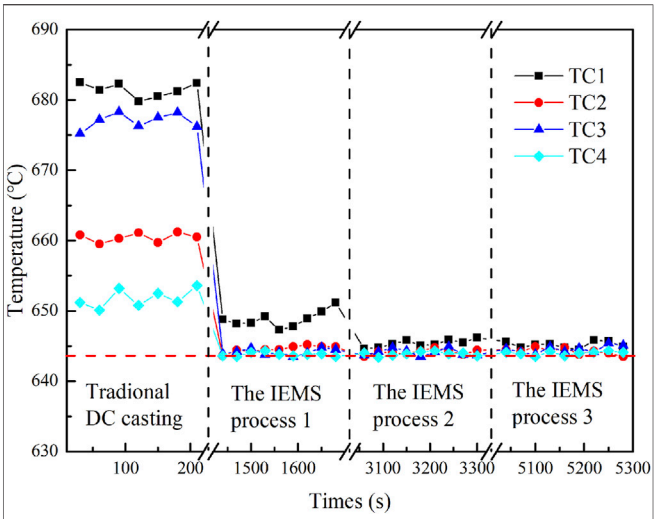

FIGURE 6 | Temperature–time curves as the casting condition changes.

the melt in turn. The Lorentz Force in the melt, $\boldsymbol{F}$, is represented in the following equation:

$$\boldsymbol{F} = \boldsymbol{J} \times \boldsymbol{B} = -\frac{\mathbf{1}}{\mathbf{2}\boldsymbol{\mu}}\nabla \boldsymbol{B}^{\mathbf{2}} + \frac{\mathbf{1}}{\boldsymbol{\mu}}(\boldsymbol{B} \cdot \nabla)\boldsymbol{B},$$

where μ is the permeability of the melt, and the J and B are the induced current density and magnetic induction intensity, respectively. The second term on the right-hand side of the above equation provides a rotational component in the melt, leading to forced convection. Therefore, the higher the alternative current, the larger the Lorentz force and the induced melt flow outside the in-mold cooler. The skin effect of the magnetic field and currents is solved by the IEMS effectively and elegantly. The magnitude of the Lorentz Force decreases with increasing radial distance from the surface of the experimental in-mold cooler, and it is enough to drive the entire melt flow intensively.

Figure 6 demonstrates the temperature curves measured at different positions (TC1, TC2, TC3, and TC4 shown in **Figure 1**) in the melt during the four casting processes. It can be seen that forced convection can improve the uniformity of the temperature field in the melt. In the traditional DC casting process, the temperature differences in the sump are larger than that in the IEMS process. The observed temperatures at the mid-level of the liquid zone in the vertical direction are extremely close to the value at the bottom of the liquid zone. It can be inferred from **Figure 6** that the temperature gradient in the liquid zone is very small, and the temperature gradient in the mushy region is very large, leading to the coarse and dendritic grains in the center of the billet. With the application of the IEMS process, the temperature of the four thermocouples in the melt decreases rapidly to about 648.8, 646.5, 648.1, and 646.2°C. The forced convection drives the high-temperature melt to spread around and enhances the radial heat transfer rate, resulting in improving the uniformity of the temperature field. The lower temperature in the melt remarkably reduces the remelting of nuclei, and the depth of the liquid-solid transition region gets larger. Felmings (1991) studied the break-up of secondary arms and the remelting of the root of dendrite arms, and the nuclei increased. With the help of forced convection, a great number of the effective nuclei in the entire melt can survive, well dispersed and distributed uniformly in the entire melt, and grew up in the direction opposite the temperature gradient until hindered by another nucleus, which makes contributions to the refinement of the microstructure.

Figure 7 demonstrates the sump depths in the traditional DC casting process and the IEMS process. The depth of the liquid sump decreases from 392 to 312 mm and becomes flattered by applying the IEMS process (22 A and 20 Hz), which means that the average temperature gradient is also decreased in the horizontal direction, fitted in well with the data of the temperatures of TC2 and TC4. However, there are small changes in the sump depth after increasing the current density (42 A), but the melt temperature decreases and becomes more uniform. The average temperatures of TC1 to TC4 are all around 643.6°C, which is close to the liquidus temperature. It is clear that with increasing the current from 0 to 22 A, the structure transforms from coarse equiaxed and dendritic grains to finer and more uniform equiaxed grains. The intensive melt flow is responsible for the production and dispersion of a larger number of nuclei featured by a critical size. The significant increase of the floating nucleus density in the entire melt leads to the grain size gradually decreasing and developing into equiaxed grains in the center of the billet. When increasing the current from 22 to 42 A, the grains in the center of the billet become further fine and more uniform, but the grain size decreases slowly. In addition, with the increase of current frequency from 20 to 30 Hz, the effective nuclei in the melt cannot significantly increase although the microstructures become finer. The change in grain size is relatively small because of the stronger intensive melt flow.

It has been demonstrated in this work that the forced convection caused by the IEMS process could affect the macrosegregation. The

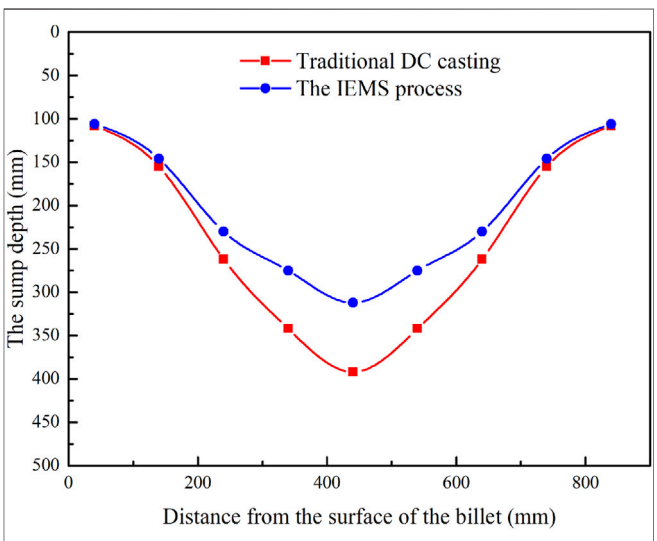

FIGURE 7 | Variation of liquid sump depths of an AA2219 billet with a diameter of 880 mm cast by DC and the IEMS processes.

segregation can be controlled by adjusting the casting electromagnetic parameters, which means that the relative movement of solid and liquid phases in the solid-liquid phase region can be affected during the casting. It is natural convection caused by the temperature and concentration gradients, also known as thermo-solutal nature melt flow, in the traditional DC casting. The melt in the periphery cooled faster than that in the bottom of the liquid sump, and there is a temperature difference between the different portions of the billet. Therefore, the lower-temperature melt at the periphery sinks along the solidification front and forces the high-temperature melt liquid in the center to rise to the hot top. At the same time, the solute-rich liquid is brought to the liquid sump and mixed with the bulk liquid from the hot top, and then the composition of the Cu alloy element is enriched when the melt in this portion of the billet begins to solidify. Meanwhile, the same solute-lean floating grains may sink into the bottom of the liquid sump, which resulted in coarse grains and negative segregation in the central portion of the billet. At the end of solidification, the shrinkage-induced flow causes negative segregation in the central portion of the billet too (Nadella et al., 2008). The result of macrosegregation at this position is determined by the combined action of the aforementioned ways. In the casting of a large-sized AA2219 billet, the thermo-solutal nature of convection plays a major role in the formation of macrosegregation. With the application of the IEMS process, the direction of melt flow changes and is enhanced into an intensive rotational flow, and the liquid sump becomes shallower and flatter. The solute is well mixed due to stirring action and the thermo-solutal nature of melt flow in the slurry zone is suppressed in the presence of the IEMS process. And the positive segregation in the billet is compensated and then reversed to the slight negative segregation. However, when the current increased to 42 A, the stronger forced flow facilitated the penetration of the solute-rich liquid coming from the central part of the sump to the edge, which strengthened the contribution of shrinkage-induced flow and floating grains. By increasing the applied current frequency, the results show that the area of negative segregation decreases to some extent, which is very important for the high quality of the billet. Further experimental trials are going to be conducted to confirm this effect and understand its mechanism.

CONCLUSION

The IEMS process can significantly refine the grain size, improve the microstructure uniformity, and control the macrosegregation of the large-sized 2219 aluminum alloy billet in DC casting. A set of relevant experimental trials have been carried out to demonstrate the effect on grain refinement and macrosegregation control. The intensity of melt flow driven by the internal electromagnetic field plays a great role in the formation of grain structure. A refinement of the grain size and more homogeneous distribution in the grain size on the large-sized AA2219 billet as the current intensity increases. Compared with the traditional DC casting, the IEMS process reverses the positive segregation in the center of the billet into slight negative segregation, but with the increase of the current intensity, it induces a more severe negative segregation. The IEMS process with proper parameters can provide a feasible method to control the macrosegregation for the preparation of large-sized, high-quality aluminum alloy billets with a fine and uniform grain structure.

DATA AVAILABILITY STATEMENT

The original contributions presented in the study are included in the article/Supplementary Material, further inquiries can be directed to the corresponding authors.

AUTHOR CONTRIBUTIONS

Conceptualization, ZZ, BL, YB, HZ, and MG; methodology, ZZ, HZ, and MG; validation, ZZ and YB; investigation, ZZ and MG; data curation, HZ; writing—original draft preparation, HZ; writing—review and editing, ZZ, BL, and YB; supervision, ZZ; project administration, ZZ. All authors have read and agreed to the published version of the manuscript.

FUNDING

This research was funded by the Project of Precise Control Technology of integral forming microstructure and properties of large aerospace aluminum alloy rotating parts (No. B109), developed by GRINM Metal Composites Technology Co., Ltd.

ACKNOWLEDGMENTS

The authors are grateful to Xinjiang Joinworld Company Limited for their help in the DC casting work.

REFERENCES

An, L., Cai, Y., Liu, W., Yuan, S., Zhu, S., and Meng, F. (2012). Effect of Pre-deformation on Microstructure and Mechanical Properties of 2219 Aluminum alloy Sheet by Thermomechanical Treatment. *Trans. Nonferrous Met. Soc. China* 22, 370–375. doi:10.1016/s1003-6326(12)61733-6

Cao, Z., Jia, F., Zhang, X., Hao, H., and Jin, J. (2002). Microstructures and Mechanical Characteristics of Electromagnetic Casting and Direct-Chill Casting 2024 Aluminum Alloys. *Mater. Sci. Eng. A.* 327, 133–137. doi:10.1016/S0921-5093(01)01673-2

Eskin, D. (2008). Effect of Different Grain Structures on Centerline Macrosegregation during Direct-Chill Casting. *Acta Materialia* 56, 1358–1365. doi:10.1016/j.actamat.2007.11.021

Felmings, M. (1991). Behavior of Metal Alloys in Semi-solid State. *Metall. Mater. Trans. A.* 22, 957–981.

Jha, A. K., Murty, S. V. S. N., Sreekumar, K., and Sinha, P. P. (2009). High Strain Rate Deformation and Cracking of AA 2219 Aluminium alloy Welded Propellant Tank. *Eng. Fail. Anal.* 16, 2209–2216. doi:10.1016/j.engfailanal.2009.03.001

Liu, X.-d., Zhu, Q.-f., Li, Z.-m., Zhu, C., Wang, R., Jia, T., et al. (2021). Effect of Casting Speed on Floating Grains and Macrosegregation of Direct-Chill Cast

2024 alloy with Intensive Melt Shearing. *Trans. Nonferrous Met. Soc. China* 31, 565–575. doi:10.1016/s1003-6326(21)65519-x

Liu, X., Zhu, Q., Zuo, Y., Zhu, C., Zhao, Z., and Cui, J. (2019). Effect of the Intensity of Melt Shearing on the as Cast Structure of Direct Chill Cast 2024 Aluminum alloy. *Metall. Mater. Trans. A.* 50, 5727–5733. doi:10.1007/s11661-019-05452-1

Luo, Y., Zhang, Z., Gao, M., Li, B., and Chen, C. (2018). Control of Microstructure and Macrosegregation of Large-Sized Aluminium alloy Billet by Uniform Direct Chill Casting. *Int. J. Cast Met. Res.* 32, 31–35. doi:10.1080/13640461.2018.1507159

Luo, Y., Zhang, Z., Li, B., Gao, M., Qiu, Y., and He, M. (2017). Effects of Annular Electromagnetic Stirring Coupled with Intercooling on Grain Refinement and Homogeneity during Direct Chill Casting of Large-Sized 7005 alloy Billet. *JOM* 69, 2640–2643. doi:10.1007/s11837-017-2340-8

Luo, Y., and Zhang, Z. (2019). Numerical Modeling of Annular Electromagnetic Stirring with Intercooling in Direct Chill Casting of 7005 Aluminum alloy Billet. *Prog. Nat. Sci. Mater. Int.* 29, 81–87. doi:10.1016/j.pnsc.2019.01.007

Mao, X., Yi, Y., He, H., Huang, S., and Guo, W. (2020). Second Phase Particles and Mechanical Properties of 2219 Aluminum Alloys Processed by an Improved Ring Manufacturing Process. *Mater. Sci. Eng. A* 781, 139226. doi:10.1016/j.msea.2020.139226

Mapelli, C., Gruttadauria, A., and Peroni, M. (2010). Application of Electromagnetic Stirring for the Homogenization of Aluminium Billet Cast in a Semi-continuous Machine. *J. Mater. Process. Tech.* 210, 306–314. doi:10.1016/j.jmatprotec.2009.09.016

Nadella, R., Eskin, D. G., Du, Q., and Katgerman, L. (2008). Macrosegregation in Direct-Chill Casting of Aluminium Alloys. *Prog. Mater. Sci.* 53, 421–480. doi:10.1016/j.pmatsci.2007.10.001

Qiu, Y., Zhang, Z., Luo, Y., Gao, M., Li, B., and Chen, C. (2018). Effect of Coupled Annular Electromagnetic Stirring and Intercooling on the Microstructures, Macrosegregation and Properties of Large-Sized 2219 Aluminum alloy Billets. *Int. J. Mater. Res.* 109, 469–475. doi:10.3139/146.111620

Qiu, Y., Zhang, Z., and Zhao, H. (2019). Internal Electromagnetic Stirring Method for Preparing a Large-Sized Aluminum alloy Billet. *Int. J. Mater. Res.* 110, 1083–1086. doi:10.3139/146.111842

Subroto, T., Eskin, D. G., Beckwith, C., Skalicky, I., Roberts, D., Tzanakis, I., et al. (2020). Structure Refinement upon Ultrasonic Melt Treatment in a DC Casting Launder. *JOM* 72, 4071–4081. doi:10.1007/s11837-020-04269-3

Tonry, C. E. H., Bojarevics, V., Djambazov, G., and Pericleous, K. (2020). Contactless Ultrasonic Treatment in Direct Chill Casting. *JOM* 72, 4082–4091. doi:10.1007/s11837-020-04370-7

Vives, C. (1989). Electromagnetic Refining of Aluminum Alloys by the CREM Process: Part I. Working Principle and Metallurgical Results. *Mtb* 20, 623–629. doi:10.1007/bf02655919

Vives, C., and Ricou, R. (1985). Experimental Study of Continuous Electromagnetic Casting of Aluminum Alloys. *Mtb* 16, 377–384. doi:10.1007/bf02679730

Wang, X.-j., Cui, J.-z., Zuo, Y.-b., Zhao, Z.-h., and Zhang, H.-t. (2011). Effects of Low-Frequency Electromagnetic Field on the Surface Quality of 7050 Aluminum alloy Ingots during the Hot-Top Casting Process. *Int. J. Miner. Metall. Mater.* 18, 165–168. doi:10.1007/s12613-011-0417-x

Zhang, B., Cui, J., and Lu, G. (2003). Effects of Low-Frequency Electromagnetic Field on Microstructures and Macrosegregation of Continuous Casting 7075 Aluminum alloy. *Mater. Sci. Eng. A* 355, 325–330. doi:10.1016/s0921-5093(03)00105-9

Zhang, L., Li, X., Liu, Z., Li, R., Jiang, R., Guan, S., et al. (2021). Scalable Ultrasonic Casting of Large-Scale 2219aa Al Alloys: Experiment and Simulation. *Mater. Today Commun.* 27, 102329. doi:10.1016/j.mtcomm.2021.102329

Zhao, Z.-h., Xu, Z., Wang, G.-s., Zhu, Q.-f., and Cui, J.-z. (2014). As-cast Structure of Dc Casting 7075 Aluminum alloy Obtained under Dual-Frequency Electromagnetic Field. *Int. J. Miner. Metall. Mater.* 21, 150–154. doi:10.1007/s12613-014-0878-9

Zuo, Y.-b., Cui, J.-z., Mou, D., Zhu, Q.-f., Wang, X.-j., and Li, L. (2014). Effect of Electromagnetic Field on Microstructure and Macrosegregation of Flat Ingot of 2524 Aluminium alloy. *Trans. Nonferrous Met. Soc. China* 24, 2408–2413. doi:10.1016/s1003-6326(14)63364-1

Zuo, Y., Liu, X., Sun, C., Yuan, S., Mou, D., Li, Z., et al. (2015). Grain Refinement and Macrosegregation Behavior of Direct Chill Cast Al-Zn-Mg-Cu alloy under Combined Electromagnetic fields. *China Foundry* 12, 333–338. doi:10.5455/medarh.2015.69.10-12

Conflict of Interest: Authors HZ, ZZ, BL, YB, and MG were employed by the company GRINM Metal Composites Technology Co., Ltd.

Publisher's Note: All claims expressed in this article are solely those of the authors and do not necessarily represent those of their affiliated organizations, or those of the publisher, the editors, and the reviewers. Any product that may be evaluated in this article, or claim that may be made by its manufacturer, is not guaranteed or endorsed by the publisher.